EMBEDDED MULTIPLE DESCRIPTION SCALAR QUANTIZERS FOR PROGRESSIVE IMAGE TRANSMISSION

A. I. Gavrilescu, A. Munteanu, P. Schelkens, J. Cornelis

Vrije Universiteit Brussel
Department of Electronics and Information Processing (ETRO)
Pleinlaan 2, B-1050 Brussels, Belgium
* Email: aigavril@etro.vub.ac.be

ABSTRACT

Robust progressive image transmission over unreliable channels with variable bandwidth requires Multiple Description Coding (MDC) systems that produce highly error-resilient embedded bit-streams. The proposed Embedded Multiple Description Scalar Quantizers (EMDSQ) meet the desired features consisting of a high redundancy level, fine grain rate adaptation and progressive transmission of each description. Experimental results show that EMDSQ yield better rate-distortion performance in comparison to the Multiple Description Uniform Scalar Quantizers (MDUSQ) previously proposed in the literature. Moreover, the generalized form of EMDSQ targeting an arbitrary number of channels is proposed, which offers the possibility of designing realistic coders for practical multi-channel communication systems.

1. INTRODUCTION

A new family of communication services involving the delivery of image data over bandwidth limited and error prone channels as packet networks and wireless links has emerged in the last few years. In order to increase the reliability over these types of channels, diversity is commonly resorted to, besides error correction techniques. Multiple Description Coding was introduced to efficiently overcome the channel impairments over diversity-based systems allowing the decoders to extract meaningful information from a subset of a bit-stream.

The focus of previous research was laid on finding the optimal achievable rates-distortion regions in [1], [2], followed by the design of practical compression systems to meet these theoretical boundaries. Examples include methods based on quantization [3], [4] and multiple description transform [5], [6]. The design of multiple description scalar quantizers (MDSQ) was pioneered in [3] under the assumption of fixed length codes and fixed codebook sizes. Significant improvements are achieved in [4] where the design of the quantizers is subject to the constraint of a given entropy, and not of a given codebook size.

In order to achieve robust communication over unreliable channels the MDC system has to deliver highly error-resilient bit-streams characterized by a corresponding high level of redundancy. Additionally, a fine grain scalability of the bit-stream is a desirable feature for bandwidth varying channels. A system conceived so as to meet these requirements is described in [7] where the progressive MDC algorithm is based on multiple description uniform scalar quantizers (MDUSQ). Moreover, for a high level of redundancy and for low bit-rates, the approach of [7] outperforms the embedded MDC algorithm based on the polyphase transform proposed in [8].

In this paper we introduce another type of embedded scalar quantizers for MDC systems, which we shall refer to as Embedded Multiple Description Scalar Quantizers (EMDSQ). The proposed EMDSQ meet the desired features consisting of a high redundancy level, fine grain rate adaptation and progressive transmission of each description. For an erasure channel model characterized by burst errors, progressive transmission shall also provide quality improvement for the central reconstruction due to the use of undamaged data from partially damaged received side channels. The reconstruction of the central channel can be performed if the receiver knows where the burst error occurs. To satisfy this requirement, techniques such as inserting synchronization markers in the bit-stream can be used.

The above-mentioned MDUSQ [7] and the proposed EMDSQ are incorporated in a wavelet-based coding system that employs the Quad Tree (QT) coding algorithm described in [9]; the rate-distortion performances of both MDC systems are compared, when applied on a common dataset. Finally, the generalized form of EMDSQ targeting an arbitrary number of channels is proposed, offering the possibility of designing realistic coders for practical multi-channel communication systems.

The paper is structured as follows. In Section 2 the proposed EMDSQ are introduced. Section 3 describes briefly the coding system based on QT coding. Comparative coding results are given in Section 4. Finally, we conclude our work in Section 5.

2. EMBEDDED MULTIPLE DESCRIPTION SCALAR QUANTIZERS

The system proposed by Vaishampayan [3] relies on the ability to design scalar quantizers with nested thresholds. The source represented by a random process $\{X_n, \ n \in \mathbb{Z}_+ \}$ with zero mean and variance σ_X^2 is quantized by the side quantizers $Q_S^m : R \to \{0,1,...,K\text{-}1\}$, $m = 1,2$. Each of the two quantizers outputs an index $q_k^m, k \in \mathbb{Z}_+$ that can be separately used to estimate the source sample. The reconstruction where $Q_S^m(x) = q_k^m$ must be the centroid of the cell $Q_S^{m^{-1}}(q_k^m)$. If both indices $Q_S^1(x) = q_k^1$ and $Q_S^2(x) = q_k^2$ are received, the reconstruction is the centroid of the intersection $Q_C^{-1}(q_k^1, q_k^2) = Q_S^{1^{-1}}(q_k^1) \cap Q_S^{2^{-1}}(q_k^2)$ represented by the central inverse quantizer. The number of diagonals covered in the index assignment matrix triggers the redundancy between the two descriptions [3].

Quantization methods based on embedded scalar quantizers were previously proposed in the literature – see for e.g. [10]. In embedded quantization, the partition cells at higher quantization rates are embedded in the partition cells at lower rates. We assume a set of embedded side quantizers $Q_S^{m,0}$, $Q_S^{m,1}$,..., $Q_S^{m,P}$ with $m = 1,2$, and a set of embedded central quantizers Q_C^0, Q_C^1, ..., Q_C^P where $Q_C^{p^{-1}}(q_k^1, q_k^2) = Q_S^{1,p^{-1}}(q_k^1) \cap Q_S^{2,p^{-1}}(q_k^2)$ for any quantization level p, $0 \le p \le P$. The partition cells of any quantizer $Q_S^{m,p}$ and Q_C^p are embedded in the partition cells of the quantizers $Q_S^{m,P}$, $Q_S^{m,P-1}$,..., $Q_S^{m,p+1}$ and Q_C^P, Q_C^{P-1},..., Q_C^{p+1} respectively.
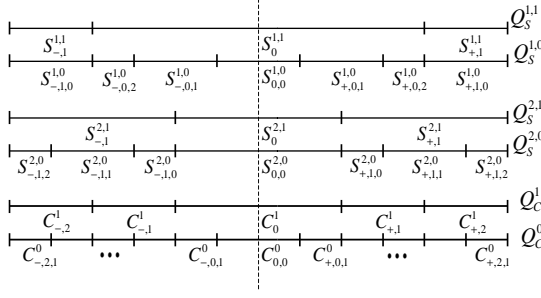
Fig. 1. Two-channel EMDSQ. The two side quantizers are $Q_S^{m,p}$, with $m=1,2$ and $p=0,1$. $Q_C^p(x)$ represents the central quantizer. Neglecting the signs, the side and central partitions cells are of the form $S_{k_0}^{m,1}$, $S_{k_0,k_1}^{m,0}$ and $C_{k_0}^1$, C_{k_0,k_1}^0, respectively.

Denote by N the number of cells of $Q_S^{m,P}$ and by L_k the number of partitions in which an arbitrary side partition cell $S_k^{m,p}$ of $Q_S^{m,p}$ is divided. The maximum number of cells in which any $S_k^{m,p}$ is partitioned is denoted by N_p, with $L_k \le N_p$ for any k. Starting from the lowest-rate quantizer $Q_S^{m,P}$, each side partition cell $S_{k_P}^{m,P}$, $0 \le k_P < N$ is divided into a number of L_{k_P} cells $S_{k_P,k_{P-1}}^{m,P-1}$, $0 \le k_{P-1} < L_{k_P}$ of $Q_S^{m,P-1}$. In general, for each side-quantizer $Q_S^{m,p}$ one associates to any $X \in S_{k_P,k_{P-1},...,k_p}^{m,p}$ the quantizer index $k_P, k_{P-1},...,k_p$. This allows us to obtain the indices of lower rate quantization by leaving aside components of higher rate quantization, similar to the uniform embedded scalar quantizers [10].

For the proposed EMDSQ family, the side quantizers $Q_S^{m,p}$ are non-uniform embedded quantizers, thus for any $0 \le p \le P$ there exist k, j, $k \ne j$ such that $L_k \ne L_j$. The example depicted in Fig. 1 illustrates an instantiation of the proposed two-channel EMDSQ. In view of simplification, we consider only two quantization levels $p=0,1$. We notice for instance that the partitions $S_{-1}^{2,1}$ and $S_{+1}^{2,1}$ of the second-channel embedded quantizer $Q_S^{2,1}$ are divided respectively into the three partitions $S_{\pm1,0}^{2,0}$, $S_{\pm1,1}^{2,0}$ and $S_{\pm1,2}^{2,0}$ of the higher rate quantizer $Q_S^{2,0}$. On the contrary, the dead zone $S_0^{2,1}$ is not divided and is transformed into $S_{0,0}^{2,0}$ of $Q_S^{2,0}$.

A uniform entropy-coded scalar quantizer is optimal for high rates, and nearly optimal for lower rates [10]. Furthermore, for input data with symmetric probability density function (PDF), the rate-distortion behavior at low rates can be improved by widening the partition cell located around zero, that is, by using deadzone uniform scalar quantizers [10]. It can be noticed that the central quantizer obtained from the side quantizers presented in Fig. 1 is a double-deadzone embedded quantizer. Hence, it shows the abovementioned characteristics.

For two-channel EMDSQ, the analytical expression of the proposed embedded side-quantizer for the first channel is:

$$Q_S^{1,p}(x)=\begin{cases} 0 & x\in[-A_{Inf}^{1,p},A_{Inf}^{1,p}) \\ Q_A^{1,p}(x) & x\in\left[-A_{Sup}^{1,p},-A_{Inf}^{1,p}\right)\cup\left[A_{Inf}^{1,p},A_{Sup}^{1,p}\right) \\ Q_B^{1,p}(x) & x\in\left[-B_{Sup}^{1,p},-B_{Inf}^{1,p}\right)\cup\left[B_{Inf}^{1,p},B_{Sup}^{1,p}\right) \end{cases} \quad (1)$$

where:

$$Q_A^{1,p}(x)=sign(x)\left(\left\lfloor\frac{|x|}{2^p\Delta}+\frac{\xi}{2^p}\right\rfloor-(k+p\%2)\right) \quad (2)$$

$$Q_B^{1,p}(x)=sign(x)\left(\left\lfloor\frac{|x|}{2\cdot2^p\Delta}+\frac{\xi}{2\cdot2^p}+\frac{k+(1-p\%2)}{2}\right\rfloor\right) \quad (3)$$

The boundary points in (1) are defined as follows:

$$A_{Sup}^{1,p}=\Delta(2^p(3k+1+2p\%2)-\xi), \quad A_{Inf}^{1,p}=\Delta(2^p(3k+2p\%2)-\xi),$$

$$B_{Sup}^{1,p}=\Delta(2^p(3k+3-p\%2)-\xi), \quad B_{Inf}^{1,p}=\Delta(2^p(3k+1-p\%2)-\xi).$$

where $\lfloor a \rfloor$ denotes the integer part of a, $\Delta>0$ is the cell size for Q_C^0, $p\%2=p-2\cdot\lfloor p/2\rfloor$, and ξ (with $\xi<1$) determines the width of the deadzone. The index $k\in\mathbb{Z}_+$ determines the width of the quantizer granular region.

Since the parameter ξ controls the width of the central deadzone, by tuning its value, we obtain corresponding families of embedded quantizers. It should be noted that, when $\xi=1/2$, the central quantizer is uniform, while when $\xi=0$, the deadzone width is 2Δ; this case is exemplified in Fig. 1. Negative values of the parameter ξ are further widening the deadzone [10].

2.1. Generalization to M channels EMDSQ

Vaishampayan's method to design MDSQ for two channels relies on generating 2D index allocation matrices. The index allocation method can be generalized to more than two channels and more than two receivers, respectively. Hence, the solution for an arbitrary number of channels M consists in generating an M-dimensional index allocation matrix. It is obvious that such an M-dimensional matrix can no longer be graphically represented, as in [3], and that M channel quantizers can only be formulated analytically.

Taking as a starting point equation (1) that describes the first channel quantizer corresponding to the two-channel EMDSQ, it is possible to generalize the analytical formula for M-channels, as shown below:

$$Q_S^{m,p}(x)=\begin{cases} Q_A^{m,p}(x) & x\in\left[-A_{Sup}^{m,p},-A_{Inf}^{m,p}\right)\cup\left[A_{Inf}^{m,p},A_{Sup}^{m,p}\right) \\ Q_B^{m,p}(x) & x\in\left[-B_{Sup}^{m,p},-B_{Inf}^{m,p}\right)\cup\left[B_{Inf}^{m,p},B_{Sup}^{m,p}\right) \end{cases} \quad (4)$$

with:

$$Q_A^{m,p}(x)=sign(x)\left\lfloor\frac{|x|}{mM^p\Delta}-\frac{M+1-2m}{m}(k+p\%2)\right\rfloor$$

$$Q_B^{m,p}(x)=sign(x)\left\lfloor\frac{|x|}{(M+1-m)M^p\Delta}+\frac{M+1-2m}{M+1-m}(k+1-p\%2)\right\rfloor \quad (5)$$

and the boundary points are defined as follows:

$$A_{Sup}^{m,p}=\Delta\cdot M^p((M+1)k+m+(M+1-m)(p\%2)),$$

$$A_{Inf}^{m,p}=\Delta\cdot M^p((M+1)k+(M+1-m)(p\%2)),$$

$$B_{Sup}^{m,p}=\Delta\cdot M^p((M+1)k+M+1-m(p\%2)),$$

$$B_{Inf}^{m,p}=\Delta\cdot M^p((M+1)k+m-m(p\%2)),$$

where m, $1\le m\le M$ denotes the channel index.

Notice that the particular example of (1) is derived from (4) for $M=2$, $m=1$ and $\xi=0$.

Based on the expressions for $A_{Sup}^{m,p}$, $B_{Sup}^{m,p}$, $A_{Inf}^{m,p}$, $B_{Inf}^{m,p}$ given above, one notices that the cell size $\Delta^{(p)}$ for the side quantizer $Q_S^{m,p}$ at level p and index m depends on the number of channels M by $\Delta^{(p)}=M^p\Delta^{(0)}$, where $\Delta^{(0)}$ is the cell size for the highest-rate side quantizer $Q_S^{m,0}$, and $\Delta^{(0)}=m\Delta$ or $\Delta^{(0)}=(M+1-m)\Delta$.

Fig. 2 depicts the case of four channels ($M=4$) and two quantization levels ($0\le p\le1$). Notice that the partitions of the side quantizers $Q_S^{m,0}$, $1\le m\le4$ are embedded respectively in the partitions of the side quantizers $Q_S^{m,1}$. Notice that the central quantizer Q_C^p is a double deadzone embedded quantizer with cell size $\Delta_C^{(p)}=4^p\Delta_C^{(0)}$, where $\Delta_C^{(0)}=\Delta$ is the cell size of Q_C^0.
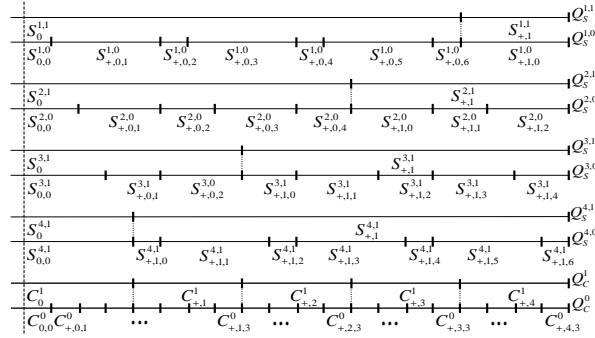
Fig. 2. Four-channel EMDSQ. The side quantizers are $Q_S^{m,p}$, with $m = 1...4$, $p = 0,1$. The central quantizer is Q_C^p. The negative side is a mirrored version of the positive side shown above.

2.2 Dependency between redundancy and the number of channels

All approaches that imply MDC involve creating redundancy in the bit-stream transmitted over several channels. Denote by $R_m, 1 \le m \le M$ the rates, and by $D_m(R_m)$ the corresponding side average distortions over M channels. The average distortion of the central quantizer shall be D_0. The standard source coder, i.e. the single-description coder (SDC) minimizes D_0 for a given rate R_0. Intuitively, the redundancy is the bit-rate sacrificed compared to the SDC coder in order to lower the D_m distortion. We consider a redundancy function:

$$\rho = \sum_{m=1}^{M} R_m - R_0 \qquad (6)$$

where R_0 is the lowest rate needed by any SDC in order to achieve the central D_0 distortion of the MDC. For a fixed D_0, the redundancy ranges from $(M-1)R_0$ (the bit-stream is replicated over the M channels) to 0 (the data is totally uncorrelated over the M channels).
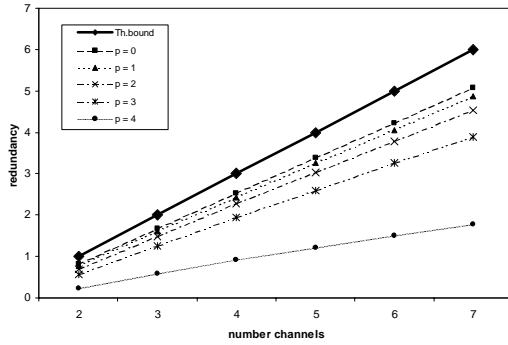

Fig. 3. Redundancy ρ versus number of channels for $2 \le M \le 7$. The number of quantization levels is $P = 5$, and $0 \le p \le 5$.

For the lowest-rate case (see example of Fig. 2), the number of central quantizer partitions is $2(M+1)-1$. Hence, the central quantizer rate is $R_0 = \log_2(2(M+1)-1)$. Since the number of partitions for all lowest-rate EMDSQ side-quantizers is three, their individual rate is $R_m = \log_2 3$. Thus, formula (6) for the lowest rate quantizers can be written $\rho_P = M \log_2 3 - \log_2(2M+1)$. Similarly, for level $p = P-1$, the number of partitions of the side quantizers $Q_S^{m,P-1}$ is $4M-1$, which yields a rate of $R_m = \log_2(4M-1)$. The central quantizer rate will be $R_0 = (\log_2 2M(M+1)-1)$. Following the same reasoning, for

quantization level p, we obtain $R_m = \log_2(4M^{P-p}-1)$ and $R_0 = \log_2(2M^{P-p}(M+1)-1)$. Consequently, the redundancy for quantization level p can be expressed as follows:

$$\rho_p = M \log_2(4M^{P-p}-1) - \log_2(2M^{P-p}(M+1)-1) \qquad (7)$$

From (7), one can deduce the analytical expression of the normalized redundancy:

$$\rho_p' = \frac{M \log_2(4M^{P-p}-1)}{\log_2(2M^{P-p}(M+1)-1)} - 1 \qquad (8)$$

One can conclude that for the EMDSQ the redundancy is directly dependent on the number of channels. Whereas, in the case of two channels, one can trigger the redundancy level by the number of diagonals filled in the index assignment matrix [3].

The graphic representation of the redundancy versus the number of channels, given by (8), is shown in Fig. 3. The theoretical boundary of the redundancy $(M-1)R_0$ is reached when the stream is replicated over M channels and is represented by the upper curve in the graph. It is noticeable that the redundancy between the channels monotonically decreases as the quantization level p increases.

3. CODING SCHEME

In this section, we illustrate the use of the proposed EMDSQ into a wavelet-based coding scheme, for the particular case of $M = 2$ and $\xi = 0$ (see Fig. 1). The coding algorithm relies on the QT coding of the significance maps [9], and is referred to as Multiple Description-QT (MD-QT) coding.
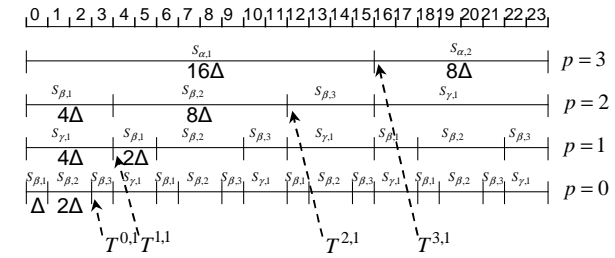

Fig. 4. Four-level representation of $Q_S^{1,p}$ for two-channel EMDSQ for an example with granular region ranging from 0 to 23. The significance map coding is performed with respect to the set of thresholds $T^{p,1}$ with the rate of decay given by (10).

The algorithm determines the significance of the coefficients with respect to a predefined set of thresholds $T^{p,m}$, which are determined for each quantization level p, $0 \le p \le P$ and channel index m, $1 \le m \le 2$. For each channel, the starting thresholds $T^{P,m}$ are of the form $T^{P,1} = 2T$ and $T^{P,2} = T$ respectively. Since it is not desirable that the quantizer is characterized by an overload region, the T value is related to the highest absolute magnitude w_{max} of the wavelet coefficients as follows:

$$T = 2^{\lfloor \log_2(w_{max}/3) \rfloor + 1} \qquad (9)$$

Hence, the maximum number of quantization levels is $P = \lfloor \log_2(w_{max}/3) \rfloor + 1$. In general, the thresholds used for each channel m, $1 \le m \le 2$ are given by:

$$T^{P-x,m} = \frac{T^{P-x+1,m}}{4^{((x+m-1)\%2)} \, 3^{((x+2-m)\%2)}} 3^{((x+m-1)\%2)} \qquad (10)$$

with $P - x = p$.

Fig. 4 depicts the thresholds $T^{p,1}$ corresponding to the first channel EMDSQ ($m=1$) for an example with granular region ranging from 0 to 23.

4. EXPERIMENTAL RESULTS

To perform the comparison between the EMDSQ and MDUSQ [7], both quantizers are applied on a memoryless Laplacian source of random generated numbers with zero mean and $\sigma = 14.6$, simulating a wavelet subband. Fig. 5 shows that comparable results are obtained for the side channel(s) and that the EMDSQ outperforms MDUSQ for the central channel. Similar experimental results were obtained varying the standard deviation within the range $12 < \sigma < 90$.
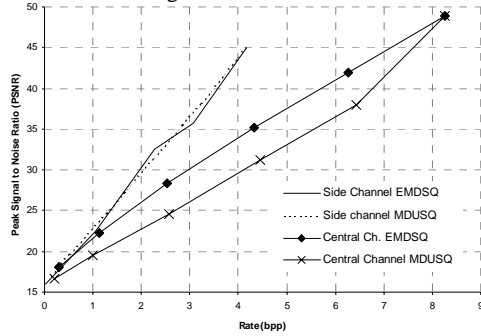

Fig. 5. Comparative side and central rate-distortion performance between EMDSQ and MDUSQ. The quantizers are applied on a 256x256 matrix of Laplacian random generated numbers with zero mean and $\sigma = 14.6$.
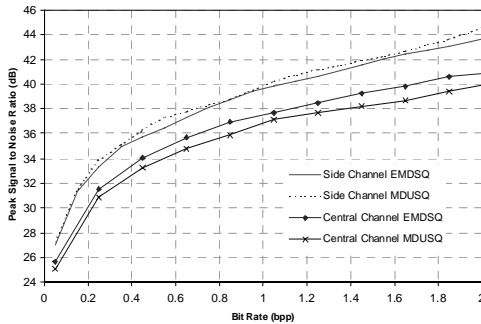

Fig. 6. Comparative side and central rate-distortion performance obtained on Lena 512x512 with the MD-QT codec employing EMDSQ and MDUSQ respectively.

Similar to EMDSQ, the MDUSQ has been integrated in the MD-QT coding scheme, resulting into a common entropy-coding module for both types of quantizers. The results shown in Fig. 6 obtained on the Lena image reveal that on the central channel the EMDSQ outperforms MDUSQ with 0.52-1.08 dB. Similarly, the results obtained on a common image data set given in Table 7 show that in comparison to MDUSQ, the proposed EMDSQ provides constantly better rate-distortion performances on the central channel for all the rates.

5. CONCLUSIONS

The paper presents a new type of embedded scalar quantizers, called here EMDSQ, as well as a comparison between the former and the MDUSQ. Designed for progressive image transmission over unreliable channels, the EMDSQ fulfill the requirement of a high level of redundancy. For the targeted high level of redundancy, the EMDSQ outperform the MDUSQ for the central channel. Thus, for an erosion channel model characterized by burst errors, coding techniques based on EMDSQ will provide better rate-distortion performance.

Image	Quant.	0.125	0.25	0.5	1	2	4
barb.raw	EMDSQ	23.90	25.72	28.52	32.56	37.75	44.52
	MDUSQ	23.63	24.87	28.20	32.16	37.15	42.85
bird.raw	EMDSQ	30.98	34.31	37.94	41.46	44.82	50.04
	MDUSQ	30.15	33.40	37.15	40.66	43.78	48.88
boat.raw	EMDSQ	26.09	28.48	31.23	34.84	39.72	44.92
	MDUSQ	25.62	27.73	30.46	33.85	38.30	43.80
camera.raw	EMDSQ	23.32	25.26	28.08	31.78	37.06	44.43
	MDUSQ	22.59	24.80	27.50	30.87	36.21	43.08
mandrill.raw	EMDSQ	20.99	21.90	23.51	25.97	29.59	35.50
	MDUSQ	20.59	21.57	22.91	25.25	28.94	34.51
average mean diff.		0.54	0.66	0.61	0.76	0.91	1.25

Table 7. Performance (PSNR) of the central reconstruction of MD-QT coding based on EMDSQ and MDUSQ for bit rates ranging from 0.125 to 4 bpp.

For the particular case when an entire channel is lost, the experiments show comparable results for the side channels. Moreover, the generalization of the coder for an arbitrary number of channels leads to the possibility of designing realistic coders for practical multi-channel communication systems.

6. ACKNOWLEDGEMENTS

7. REFERENCES

[1] L. Ozarow, "On a source coding problem with two channels and tree receivers," *Bell Syst. Tech. J.*, vol. 59, pp. 1909-1921, 1980.

[2] A. A. El Gamal and T. M. Cover, "Achievable rates for multiple descriptions," *IEEE Trans. Inform. Th.*, vol. IT-28, no. 6, pp. 851-857, 1982.

[3] V. A. Vaishampayan, "Design of multiple description scalar quantizers," *IEEE Trans. Inform. Th.*, vol. 39, no. 3, pp. 821 - 834, 1993.

[4] V. A. Vaishampayan and J. Domaszewicz, "Design of entropy-constrained multiple description scalar quantizers," *IEEE Trans. Inform. Theory*, vol. 40, no. 1, pp. 245-250, 1994.

[5] J. Batllo and V. Vaishampayan, "Asymptotic performance of multiple description transform codes," *IEEE Trans. Inform. Theory*, vol. 43, no. 2, pp. 703-707, 1997.

[6] V. Goyal, J. Kovacevic, R. Arean, and M. Vetterli, "Multiple description transform coding of images," *Proc. IEEE Int. Conf. Image Proc.* ICIP'98, pp. 674-678, 1998.

[7] T. Guionnet, C. Guillemot, and S. Pateux, "Embedded multiple description coding for progressive image transmission over unreliable channels," *Proc. IEEE Int. Conf. Image Proc.*, ICIP 2001, pp. 94 - 97, 2001.

[8] W. Jiang and A. Ortega, "Multiple description coding via polyphase transform and selective quantization," *Proc. SPIE Int. Conf. Visual Comm. Image Proc.*, VCIP'99, San Jose, USA, pp. 998-1008, 1999.

[9] A. Munteanu, J. Cornelis, G. Van der Auwera, and P. Cristea, "Wavelet-based lossless compression scheme with progressive transmission capability," *Int. J. Imaging Systems and Tech.,* vol. 10, no. 1, pp. 76-85, Jan. 1999.

[10] D. Taubman and M. W. Marcellin, *JPEG2000 - Image Compression: Fundamentals, Standards and Practice.* Hingham, MA: Kluwer Academic Publishers, 2001.